Molecular composition of organic peroxides in secondary organic aerosols revealed by peroxide-iodide reactivity

Kangwei Li [1*], Zhensen Zheng [2,3], Julian Resch [1], Jialiang Ma [4], Markus Kalberer [1*]

1. Department of Environmental Sciences, University of Basel, Basel 4056, Switzerland

2. Institute of Ion Physics and Applied Physics, University of Innsbruck, Innsbruck, Austria

3. IONICON Analytik GmbH, 6020 Innsbruck, Austria

4. Institute for Atmospheric and Environmental Sciences, Goethe-University Frankfurt, Frankfurt am Main, 60438, Germany

Correspondence to: Kangwei Li (kangwei.li@unibas.ch), Markus Kalberer (markus.kalberer@unibas.ch)

Abstract

Organic peroxides are health-relevant organic components in secondary organic aerosols (SOA), which is also a major compound class substantially contributing to SOA mass. However, their molecular identification in SOA is highly challenging and uncertain. Iodide is known to selectively react with peroxides, and their kinetics are fundamentally determined by the structures of individual peroxides. Here we extrapolate this knowledge and develop a novel analytical strategy for molecular characterization of organic peroxides in α-pinene SOA via iodometry kinetic experiments, using liquid chromatography–high resolution mass spectrometry. Through non-targeted analysis, more than 300 organic peroxides are identified in α-pinene SOA with unprecedented accuracy of their chemical formula. Their reactivity with iodide is highly compound-dependent and can vary four orders of magnitude, within the range observed for some commercial organic peroxides with known structures. In particular, more than 65% of organic peroxides in α-pinene SOA exhibit a slow reactivity with iodide, with an e-folding lifetime exceeding one day. The structures of 12 organic peroxides derived from stabilized Criegee intermediates are further proposed and discussed based on different experimental evidences. Our study improves the molecular-level identification and understanding of organic peroxides in SOA, offering numerous opportunities for further investigation into their formation chemistry, atmospheric transformation, and health impact. Additionally, the peroxide-iodide reactivity is proposed as a new metric that can provide both information on the oxidizing capability and structure of individual organic peroxide in SOA.

Keywords: organic peroxide, secondary organic aerosol, LC-HRMS, iodometry, non-targeted analysis

1 Introduction

Atmospheric aerosol particles have great impact on air quality, climate change, and human health.[1] They are found everywhere in the Earth's atmosphere, present in varying composition and concentrations from remote oceanic regions and pristine wilderness areas to heavily industrialized cities. Among different aerosol components, secondary organic aerosols (SOA) are a significant component that contributing 20-90% of the total aerosol mass.[2, 3] SOA are typically formed through cascade (photo-)oxidation of volatile organic compounds (VOCs) in the atmosphere, leading to the formation of less volatile products that condense onto existing particles or nucleate to form new particles.[4] SOA consists of thousands of different organic compounds, ranging from simple molecules to highly oxidized and multifunctional species. It has been postulated that organic peroxides (ROOH and ROOR, where R denotes an organic group), a significant compound class of SOA components, may play a pivotal role in the toxicity and related health effects of aerosols.[5] This is primarily due to their reactive and oxidizing properties, where peroxides are also considered as a compound class contributing to the so-called reactive oxygen species. Despite the significance of organic peroxides in atmospheric chemistry and human health, the analytical identification and quantification of these compounds in atmospheric aerosols remains highly challenging.[6]

Iodometry is a well-established titration method for quantifying total peroxide because iodide is known to selectively react with peroxides.[5] Potassium iodide (KI) is typically added to an acidified SOA extract in a large excess (e.g. a few hundred times or more), which usually allows the total peroxides to be titrated by iodide and then fully converted to I_3^- after several hours before being quantified by UV-Vis spectroscopy. Based on such iodometry UV-Vis measurements, it has been reported that organic peroxides contribute up to 80% of SOA mass, though there is still a very large uncertainty and variation regarding the mass fraction of organic peroxides in SOA.[5] However, current molecular-level understanding of organic peroxide is still very limited due to several reasons. Firstly, a significant number of organic peroxides present in SOA remain poorly identified and characterized. This is mainly due to the chemical complexity of SOA molecular composition with diverse structures, e.g. co-existence of many peroxide and non-peroxide isomers. In particular, only about ten organic peroxide standards are commercially available, while most of them are not atmospherically relevant, in sharp contrast to a large speciation of organic peroxides present in SOA. Secondly, the atmospheric formation and transformation pathways of organic peroxides are highly complex.[7] On the one hand, numerous pathways exist by which organic peroxides can be formed, either in the gas phase or particle phase, or partitioned between the two. On the other hand, organic peroxides are reactive components, which can participate in atmospheric transformation by oxidizing or reacting with other compounds,[8] or undergo degradation due to the labile property of the -O-O- functional group.[9]

Therefore, there is a need of reliable and accurate analytical method for molecular-level identification of organic peroxide in SOA, which would allow further investigation into their formation chemistry, chemical transformation, and health impact. Recently, Zhao et al.[10] developed a novel analytical method for molecular identification of organic peroxides in SOA, which combines iodometry and liquid chromatography coupled to high-resolution mass spectrometry (LC-HRMS). Briefly, one aliquot of SOA extract was untreated, while another aliquot was dosed with concentrated KI to proceed iodometry reactions for several hours, before these two samples being injected into LC-HRMS. The organic peroxide is therefore identified if the chromatographic peak is disappeared or largely reduced in the KI-treated sample. Another study [11] further employed this method and 75 isomer-resolved organic peroxides were identified in α-pinene SOA. These previous studies indeed show iodometry-assisted LC-HRMS as a promising method for molecular identification of organic peroxides in SOA. However, the kinetics between iodide and organic peroxides should be fundamentally determined by the structure of individual peroxide, which was not yet fully recognized. An analogous example is the hydrolysis, though this is a very different type of reaction compared with iodometry. As explored in our recent study,[12] a number of structure-known α-acyloxyalkyl hydroperoxides (AAHPs, a sub-class of organic peroxide) were synthesized and their

hydrolysis kinetics were experimentally determined to be very compound-dependent. Given the very large speciation and structures as well as diverse formation pathways of organic peroxides in SOA, we hypothesize that the peroxide-iodide reactivity should also be compound- and structure-dependent, which is the main motivation of this study.

In this study, we firstly characterized the kinetics between iodide and individual peroxide standards that are commercially available, which allows us to recognize the range and importance of peroxide-iodide reactivity. Then, we performed iodometry kinetic experiments for α-pinene SOA based on iodometry-assisted LC-HRMS and non-targeted analysis, where more than 300 organic peroxides were unambiguously identified with precise formula information, and extended structure information was further revealed by peroxide-iodide reactivity. Our results expand the molecular-level identification and understanding of organic peroxides in SOA, which represents a fundamental step and prerequisite for future investigation of their formation chemistry, atmospheric transformation, and health impact.

2 Method

2.1 Chemicals

All the 11 commercial peroxide standards were bought from Sigma-Aldrich, including hydrogen peroxide (H_2O_2, 30%), peracetic acid (PAA, 36-40%), 3-chloroperbenzoic acid (3-CA, 77%), benzoyl peroxide (BP, with 25% H_2O), tert-butyl hydroperoxide (t-BH, 70%), cumene hydroperoxide (CH, 80%), tert-butyl peroxybenzoate (t-BPB, 95%), tert-butyl peracetate (t-BPA, 50%), tert-butyl peroxide (t-BP, 98%), dicumyl peroxide (DP, 98%), and 2-butanone peroxide (2-BP, 32%). Additional chemicals used in this study include α-pinene (98%, Sigma-Aldrich), potassium iodide (KI, 99.5%, Sigma-Aldrich), acetonitrile (ACN, Optima LC/MS grade, Fisher Scientific), methanol (Optima LC/MS grade, Fisher Scientific), formic acid (Optima LC/MS grade, Fisher Scientific), acetic acid (Optima LC/MS grade, Fisher Scientific), camphorsulfonic acid (98%, Sigma-Aldrich), cyclohexane (99%, Sigma-Aldrich), and water (Optima LC/MS grade, Fisher Scientific).

2.2 Laboratory-generated SOA and filter extraction

Ten different α-pinene SOA samples were collected from flowtube experiments by mixing α-pinene vapor (in ppm level) with O_3 in the dark under various conditions. The formed SOA particles were collected onto 47 mm PTFE membrane filters (0.2 μm pore size, Whatman) with a known mass loading (~200 μg). Figure S1 shows the flowtube setup, which incorporates a recently developed instrument, namely organic coating unit,[13] for the precise and consistent generation of VOC vapor prior to its mixing with ozone. These flowtube experiments were conducted under a wide range of conditions, including variations in initial ozone concentrations (0.5–25 ppm), humidity (0–80%), and with or without the addition of cyclohexane as an OH scavenger. After collection, one-fourth of the filter was dosed with 20 μL of 5 μM camphorsulfonic acid as an internal standard, and then immediately extracted by acetonitrile (ACN). The extracts were then concentrated to complete dryness (Eppendorf Concentrator plus, Fisher Scientific) and reconstituted with 150 μL of ACN before being injected into LC-HRMS. We intentionally use ACN as extraction solvent to minimize other unwanted decomposition processes such as hydrolysis, as good stability of AAHPs in ACN have been observed in our recent study.[12] For the later on SOA iodometry kinetic experiments (as described in Section 2.5), ten extracts from ten different α-pinene SOA samples were combined as one extract, which should be highly representative as it reflects many different α-pinene SOA generating conditions on average.

2.3 Synthesis of organic peroxide standards from liquid-phase ozonolysis experiments

The ozonolysis of alkenes generates a type of reactive intermediates, stabilized Criegee intermediates (SCIs), which can further undergo various bimolecular reactions with water, alcohols, aldehydes, and carboxylic acids to form different SCI-derived organic peroxides, including α-substituted hydroperoxides and secondary ozonides (SOZ). We use an impinger

to synthesize a number of SCI-derived peroxides via liquid-phase ozonolysis. Briefly, high concentrations of O_3 (~500 ppm, 100 mL min^{-1}) was bubbled through a 10 mL ACN solution containing 1 mM α-pinene. O_3 reacted in solution with α-pinene resulting in the formation of SCIs, which were rapidly scavenged by the other co-produced oxidation products and lead the formation of SCI-derived organic peroxides. The oxidized compounds produced during the liquid-phase ozonolysis of α-pinene include various carboxylic acids, carbonyls, etc, and some of them are also expected to be formed in the gas-phase ozonolysis. At each time interval, 75 µL of solution was taken from the impinger for LC-HRMS injection, which allows to track the temporal trends of individual compounds. The temporal trend of these SCI-derived organic peroxides should follow a unique pattern that increasing in the beginning and then reaches a plateau after ca. 5 min, a critical timing when alkenes are fully consumed and SCIs are no longer available in our condition. Such a unique temporal pattern was firstly revealed in our recent study for synthesizing a number of AAHPs,[12] and here we extend this idea to synthesize a number of SCI-derived peroxides. Some of these SCI-derived peroxides are expected to be found in α-pinene SOA samples, and their structures can be further inferred based on some known formation pathways.

2.4 Liquid chromatography coupled to high-resolution mass spectrometry (LC-HRMS)

LC-HRMS consists of an ultraperformance liquid chromatography unit (ACQUITY UPLC I-Class, Waters) coupled with a high-resolution mass spectrometer (HRMS, Orbitrap Q Exactive Plus, Thermo Scientific). The detailed parameters for liquid chromatography and mass spectrometry are similar to that described in our recent study,[12] which has been summarized in Table S1. The mass spectrometer was calibrated daily for positive and negative modes using Thermo Scientific Pierce Ion Calibration Solution (Fisher Scientific), while the data presented in this study is mainly from positive mode. In addition, an HPLC Gradient System Diagnostics Mix (Sigma-Aldrich) containing five compounds was injected daily to monitor the stability of the signal intensity and retention time (RT). The extracted ion chromatograms (EICs) for selected ions were exported using Xcalibur 2.2 software (Thermo Scientific) with a mass tolerance of 10 ppm.

2.5 Iodometry kinetic experiments using UV-Vis and LC-HRMS

The first part of iodometry kinetic experiments is for those 11 peroxide standards that are commercially available. We monitor the I_3^- formation temporal pattern for each peroxide standard using a UV–Vis spectroscopy (LAMBDA 365, PerkinElmer), allowing us to determine their peroxide-iodide reactivity individually. Specifically, these peroxide standards were prepared and diluted in ACN solution at ~50 µM. Then, 1.8 mL peroxide standard (~50 µM in ACN) mixed with 0.1 mL acetic acid (600 mM in ACN) in a vial, followed by the addition of 0.1 mL KI (400 mM in H_2O). This triggers the iodometry reaction in a 2 mL solution containing ~45 µM peroxide standard, 30 mM acetic acid and 20 mM KI, which was regularly measured by UV-Vis over different time scales from minutes to up to 4 weeks. The addition of acetic acid creates an acidic condition, which provides enough protons to proceed iodometry reaction. The solution was stored in a closed vial at room temperature (~20 ℃), and its pH cannot be accurately determined because of the ACN-dominated solution.

The second part of iodometry kinetic experiments is for SOA samples, which were performed in a similar way like the above peroxide standards, where they were regularly measured by LC-HRMS instead of UV-Vis. Specifically, 40 µL was taken from each α-pinene SOA extract (150 µL initial) and finally 10 extracts were combined as 400 µL. One aliquot (180 µL) from the combined extract mixed with 10 µL acetic acid (600 mM in ACN) in a vial, followed by the addition of 10 µL KI (400 mM in H_2O) to trigger the iodometry reaction; another 180 µL aliquot was treated in a same way by adding 10 µL acetic acid (600 mM in ACN) and 10 µL H_2O, instead of KI. As shown in Table S2, these two SOA samples are designated as KI-treated and non-treated respectively, which were regularly injected into LC-HRMS for 4 weeks. Note that we directed the LC eluting flow into waste for the 0-3 min of the whole 30 min method to minimize possible contamination of KI entering into HRMS, as 20 mM KI present in the KI-

treated samples was quite high and might cause unexpected contamination. These KI-treated and non-treated SOA samples was stored in an autosampler at 8 ℃ during that four weeks, with a closed cap to avoid evaporation.

2.6 Non-targeted analysis of LC-HRMS dataset and organic peroxide identification

The LC-HRMS raw data files were converted to mzML format using the ProteoWizard (MSConvert, version 3) software and were subsequently analysed by MZmine 4.2.0.[14, 15] An optimized workflow includes mass detection, chromatogram building and deconvolution, C_{13} isotope filtering, RT alignment, feature grouping and formula prediction. The non-targeted analysis workflow and detailed parameters used in this study for MZmine are summarized in a batch file as supplementary material, which allows for reproducible LC-HRMS data processing by other MZmine users. The organic peroxide identification is based on an in-house data processing tool with graphical user interface (GUI) to allow for efficient data filtering and visualization, which are described in Text S1 and Fig. S2.

3 Results and discussion

3.1 Compound-dependent reactivity of peroxide standards with iodide

The rate constants for peroxides with iodide are mostly not available, and therefore we firstly characterize the reactivity of individual peroxide standards with iodide. 11 peroxide standards are selected, including 1 inorganic peroxide (H_2O_2) and 10 organic peroxides with diverse structures, as shown in Fig. 1. These peroxides are selected due to their commercial availability, though most of them are not atmospherically relevant. It is well known that peroxides can oxidize iodide and finally lead the formation of I_3^-, which can be easily identified by UV-Vis measurement. As mentioned in Section 2.5, we performed iodometry kinetic experiments in bulk solutions containing ~45 μM peroxide standard, 30 mM acetic acid and 20 mM KI. We monitored the I_3^- absorption as a function of time, which allows for a relative comparison of peroxide-iodide reactivity (k_{1st}) among those peroxide standards.

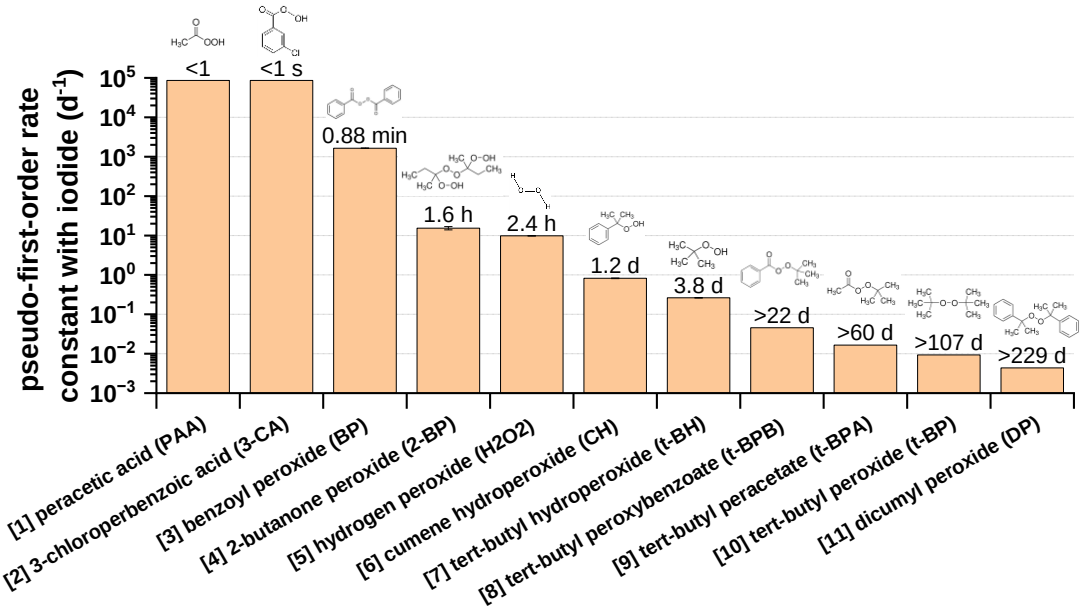

Fig. 1 Summary of peroxide-iodide reactivity (k_{1st}) for the 11 commercially available peroxides with diverse structures. The reactivity was fitted or estimated from iodometry kinetic experiments based on UV-Vis measurement, which are described and summarized in Text S2, Fig. S3 and Table S3. The reactivity for [1] PAA and [2] 3-CA were estimated as lower limit, and reactivity for [8] t-BPB, [9] t-BPA, [10] t-BP and [11] DP were estimated as upper limit. The e-folding lifetime ($\tau_{1/e}$) for each peroxide was labelled.

I_3^- has an absorption peak that typically reported within 350-353 nm in water,[16, 17] and we are aware that the I_3^- absorption peak shifts a bit to 361 nm when present in ACN-dominated solvent (i.e. 95% ACN + 5% H_2O in this study), which has been described in details in Text S2. As shown in Fig. S3, we observed large differences of I_3^- temporal profiles among these peroxide standards, which suggests a large variation of I_3^- formation rate between individual peroxide and iodide. For instance, PAA and 3-CA were fully titrated to I_3^- within less than 1 s, while the temporal I_3^- formation of some peroxides (e.g. t-BPA, t-BPB, t-BP and DP) cannot reach a plateau even after more than two weeks. Since I^- is in large excess, the k_{1st} values for these selected peroxides with iodide can be further fitted or estimated, and the calculation details are described in Text S2.

As summarized in Fig. 1 and Table S3, these peroxide standards are classified into several sub-groups, with the k_{1st} values generally following the below order: R(C=O)OOH (10^5 d^{-1}) > R(C=O)OO(C=O)R (10^3 – 10^4 d^{-1}) > ROOH ≈ H2O2 (10^{-1} – 10 d^{-1}) > R(C=O)OOR (10^{-2} – 10^{-1} d^{-1}) > ROOR (10^{-3} – 10^{-2} d^{-1}). Such compound- and structure-dependent reactivity of peroxide with iodide is reasonable and can be structurally explained by the specific position of peroxide functional group present. For example, the peroxide bond becomes more reactive when neighbouring a hydrogen atom, rather than an organic group. In addition, the presence of C=O bond next to the peroxide functional group also increases the reactivity of organic peroxides.

Among all these peroxide standards, peracids such as PAA and 3-CA show highest reactivity with iodide, which is not surprising. Generally, it is known that oxidation rate of iodide by PAA is much faster than that by H_2O_2, which leads to some spectrophotometric methods for the separate quantification of PAA and H_2O_2 when they are co-existed.[18] Despite its presence in the atmosphere,[19] PAA has also been widely applied into other fields due to its highly oxidative ability, such as advanced oxidation technology in wastewater treatment.[20] To the best of our knowledge, the available peroxide-iodide kinetic measurements are still limited to PAA and H_2O_2 with the reported aqueous rate constants differing about 4-5 orders of magnitudes (e.g. 4.22×10^2 M^{-1} s^{-1} for PAA [21] and 9.50×10^{-3} M^{-1} s^{-1} for H_2O_2 [22] that both at similar pH = 4.3), which qualitatively agrees with our observation. The measurement of k_{1st} values with such a wide range indicates an important metric, which directly links to the peroxide structures and provide sub-structural information, as explored in the next sections.

3.2 Identification of organic peroxides in SOA through non-targeted analysis

Given the above iodometry kinetic experiments from those peroxide standards, it is reasonable to assume that the kinetic of organic peroxides in SOA with iodide should also be very compound-dependent. We test this idea by performing SOA iodometry kinetic experiments, where a number of α-pinene-SOA samples were collected under different experimental conditions (see Section 2.2) and their combined extracts were divided into two aliquots. One aliquot was treated by adding concentrated KI and the other was not, and both were sequentially injected into LC-HRMS over a time scale of 4 weeks (see Section 2.5). This is regarded as an expanded method that initially proposed by Zhao et al.,[10] and we name it as time-dependent iodometry-assisted LC-HRMS.

We performed non-targeted analysis for the whole LC-HRMS dataset with an optimized workflow using MZmine 4.2.0, followed by an in-house data processing tool with GUI to efficiently visualize data and identify organic peroxides (see Section 2.6 and Fig. S2). The selection criteria for organic peroxides are described in Text S1. Fig. 2 shows several representative examples of the identified organic peroxides, including their time-dependent EICs and KI-treated/non-treated ratios. Such type of temporal pattern would allow us to identify individual organic peroxide unambiguously, especially when multiple adducts are found. For example, each suggested formula is constrained by at least two adducts and one C_{13} isotope pattern, and some adducts are matched to H_2O neutral loss (e.g. $C_{12}H_{20}O_5$ and $C_{20}H_{32}O_6$ as shown in Fig. 2A and Fig. 2C), which are all within a RT tolerance of 0.1 min and m/z tolerance of 5 ppm. Note that we are aware of the common issues of in-source fragmentation from HRMS,[23, 24] which has been taken into consideration in this study. For example, some

fragments at the same RT window can be matched to their mother ions, such as $C_{10}H_{16}O_2$ as shown in Fig. 2D, which is found unambiguously from the in-source fragmentation of $C_{20}H_{20}O_5$ that eluting at 20.7 min. All these give a level 4 identification confidence for peroxide formula assignment, according to Schymanski et al.[25]

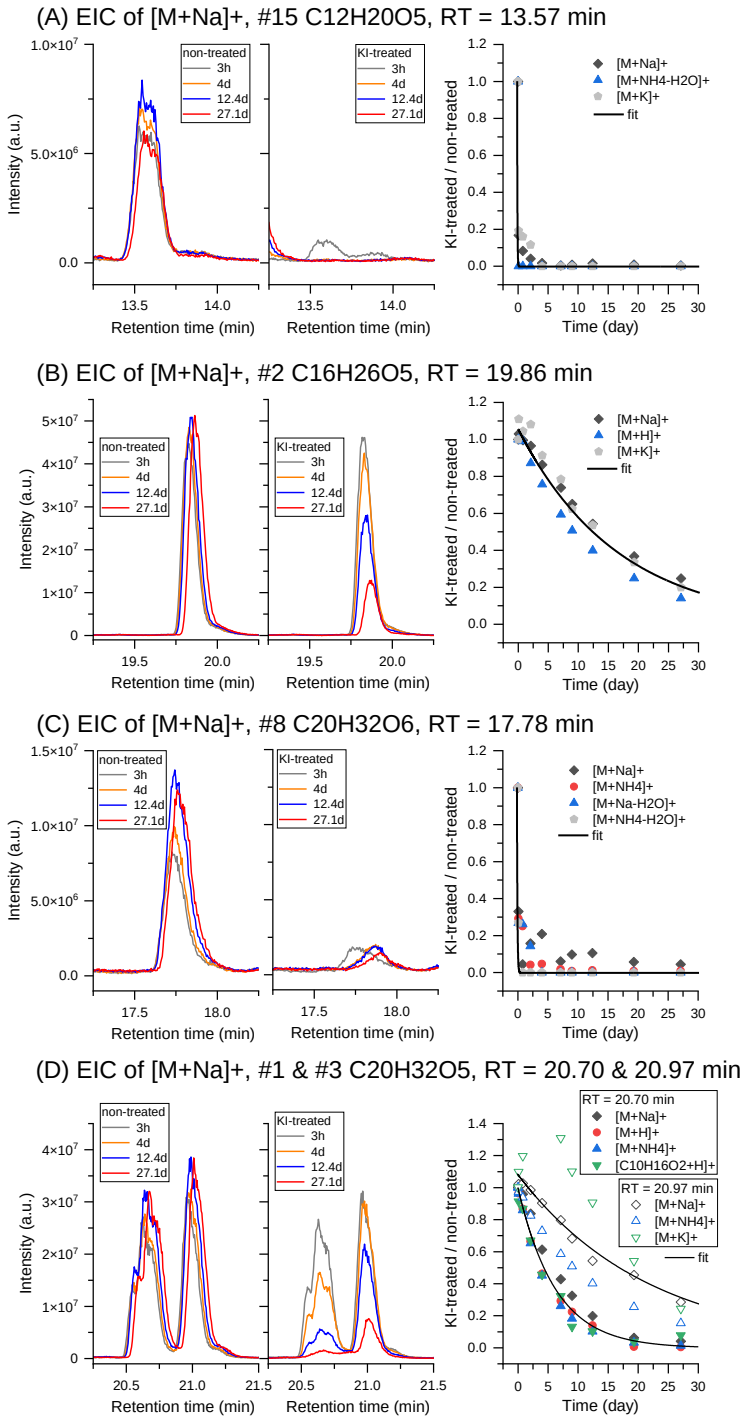

Fig. 2 Representative five organic peroxides (#1, #2, #3, #8, #15, the rank number is sorted by intensity and summarized in Table S4) identified in α-pinene SOA through time-dependent iodometry-assisted LC-HRMS. Each organic peroxide was displayed with time-dependent extracted ion chromatograms (EICs) from KI-treated and non-treated dataset, as well as temporal trends of KI-treated/non-treated ratios. The exponential fit applies to the merged data of multiple adducts from the same compound.

We use the exponential decay profile of KI-treated/non-treated ratio as a metric for k_{1st} value to determine the reactivity between organic peroxide and iodide, which rules out any other non-iodometry effects such as daily variation of instrument sensitivity, sample evaporation, etc. As shown in Fig. 2, some organic peroxides such as $C_{12}H_{20}O_5$ (RT=13.57 min) and $C_{20}H_{32}O_6$ (RT=17.78 min) show fast decay with $\tau_{1/e}$ much less than 1 day, while the relatively slow decay profile such as $C_{16}H_{25}O_5$ (RT=19.86 min) suggests $\tau_{1/e}$ of more than 10 days. Such individual decay profiles of KI-treated/non-treated ratio indicate a large reactivity difference among these selected organic peroxides, and these k_{1st} values are therefore regarded as chemical metrics that are indeed very compound-dependent. This observation is further reinforced by the reactivity difference found among isomers, where two isomers of $C_{20}H_{32}O_5$ eluting at 20.70 and 20.97 min respectively show different decay rates, which is most likely due to their different structures. Note that $C_{12}H_{20}O_5$ (RT=13.57 min) and $C_{20}H_{32}O_6$ (RT=17.78 min) are structure known AAHPs, where both of them were previously synthesized and identified in α-pinene SOA in our recent study.[12] Their successful identification in this study suggests the reliability of the new analytical method, without relying on authentic standards.

A total number of 374 organic peroxides are identified with confidence level 4 in α-pinene SOA, where the top 50 compounds are sorted by their intensity, together with their k_{1st} values and $\tau_{1/e}$ that are summarized in Table S4. Fig. 3 shows the intensity (averaged from non-treated dataset) of these organic peroxides identified in α-pinene SOA as a function of their decay rates. Among these 374 organic peroxides, they are categorized into C_6-C_{10} (n=30) as monomers, C_{11}-C_{20} (n=209) as dimers, C_{21}-C_{30} (n=130) and C_{31}-C_{40} (n=5) as higher order oligomers. It clearly shows that the intensity of these organic peroxides varies about three orders of magnitude, and their k_{1st} values differ up to four orders of magnitudes, regardless of monomeric, dimeric or oligomeric regimes. Interestingly, the error bar of the intensity reflects the variability of individual peroxide in non-treated dataset (see Table S2 for detailed constitution), which overall correlates with peroxide-iodide reactivity. For instance, these organic peroxides failing into “very slow” category tend to be less variable from the intensity. As shown in the pie chart of Fig. 3, more than 65% organic peroxides have a k_{1st} value less than 1 d^{-1} (equivalent to $\tau_{1/e}$ longer than 1 day), which further contributing more than 75% of total peroxide intensity.

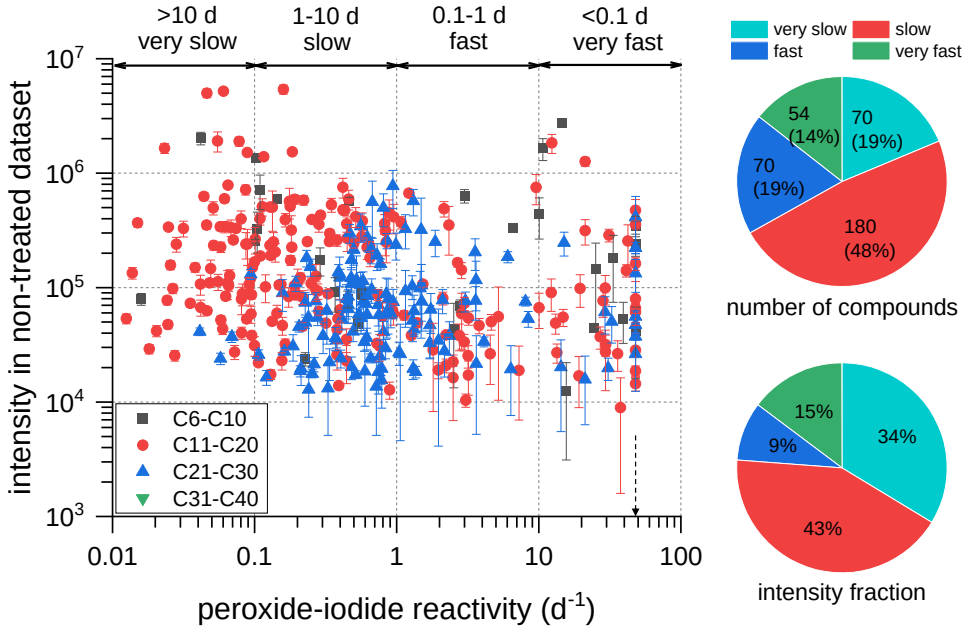

Fig. 3 Intensity of organic peroxides identified in α-pinene SOA as a function of their reactivity with iodide (k_{1st}), where the intensity and error bars reflect their average and standard deviation in the non-treated dataset (9 measurements made by LC-HRMS over four weeks). When multiple adducts present for a given organic peroxide, primary adduct was determined based on the maximum of intensity from each adduct. The number and intensity fraction of organic

peroxides are divided by their peroxide-iodide reactivity ranges as shown in the pie charts. A lower limit k_{1st} value of 48 d^{-1} ($\tau_{1/e}$ ~0.5h) was applied for some super fast-reactive peroxides, as their intensity decay to zero at the first measurement of 3 h after treating with KI and exponential fitting was therefore not possible.

The molecular composition and identification ability of organic peroxide in SOA is therefore expanded based on their wide range of reactivity with iodide. In particular, some structures and formation chemistry of organic peroxides can be qualitatively inferred based on this k_{1st} metric. For example, there are some known pathways leading to ROOH formation that likely being grouped into "fast" and "very fast" category, such as SCI-derived α-substituted hydroperoxides (e.g. AAHP), reactions between RO_2 and HO_2, and especially some autooxidation processing leading to ROOH with multiple -OOH functional group.[26] On the other hand, some known processes such as biomolecular reactions between RO_2 and RO_2, SCI and carbonyls (e.g. SOZ) can lead to ROOR formation, which are likely being grouped into "slow" and "very slow" category. Therefore, peroxide-iodide reactivity provides key information that holds great promise to further differentiate numerous formation pathways leading to organic peroxide formation.

3.3 Proposed structures of SCI-derived organic peroxides

The above results point to the fact that peroxide-iodide reactivity is strongly related to the structure of peroxides, which may be helpful for their structure elucidation. Structure characterization of organic peroxides in SOA can provide molecular-level understanding of their formation chemistry. However, accurate structure assignments for all these identified organic peroxides in SOA are not possible. Nevertheless, we may still infer some structures based on existing knowledge of organic peroxide formation chemistry.

Previous studies suggest that SCI-involved dimeric pathway is a major channel leading to the formation of organic peroxide. Here we demonstrate a simple method to synthesize a number of SCI-derived organic peroxides through liquid-phase ozonolysis experiments. Specifically, high concentrations of O_3 were bubbled through a 10 mL ACN solution containing 1 mM α-pinene, resulting in the formation of C_{10} SCIs and other oxidation products such as water, alcohols, carboxylic acids, ketones, aldehydes, etc. It is expected that SCIs should be rapidly scavenged by those co-produced oxidation products and lead the formation of SCI-derived organic peroxides, such as α-hydroxylalkyl hydroperoxides (HAHPs), α-alkoxyalkyl hydroperoxides (AHPs), AAHPs and SOZs.[5] The temporal trend of these SCI-derived organic peroxides should follow a unique pattern that increasing in the beginning and then nearly reaches a plateau after ca. 5 min, a critical timing when alkenes are fully consumed and SCIs are no longer available in our condition. Such a unique temporal pattern was firstly revealed in our recent study where AAHPs were synthesized via liquid-phase ozonolysis experiments,[12] which allows us to identify SCI-derived peroxides easily. It is expected both liquid-phase and gas-phase ozonolysis of α-pinene share many similar oxidation products, and these oxidation products are ready to be scavenged by SCIs. Therefore, some SCI-derived peroxides synthesized in the liquid-phase ozonolysis experiments are expected to be found in the α-pinene SOA samples.

As summarized in Table 1, 12 out of 374 organic peroxides found in α-pinene SOA are confirmed as SCI-derived peroxides, which is based on (i) their unique temporal trends in liquid-phase ozonolysis experiments (see Fig. S4) and (ii) their identification as organic peroxide in SOA iodometry kinetic experiments (see Fig. S5). The formula and suggested structures of their monomer partners are also summarized in Table 1, which are derived by subtracting the C_{10} SCI monomer (e.g. $C_{10}H_{16}O_3$) of α-pinene. Most of these monomers have been previously identified as oxidation products from α-pinene with reported structures, as summarized in the literatures.[27, 28] Therefore, the formation chemistry and structures of these SCI-derived peroxides can be suggested based on known formation pathways.

As shown in Table 1, most of these SCI-derived peroxides are suggested as SOZs, and their k_{1st} values (max = 0.34 d^{-1}, min = 0.042 d^{-1}) further supports their structures as SOZs. The most abundant SOZs are #1 and #3 (rank number sorted by intensity as shown in Table S4), which contribute more than 10% of total peroxide intensity. Both #1 and #3 are isomers and should have similar structures due to their close RT of 20.70 and 20.97 min, respectively. They are suggested to be formed from the bimolecular reaction between pinonaldehyde ($C_{10}H_{16}O_2$) and C_{10} SCI at confidence level 2, depending on boning to C=O or -CHO of pinonaldehyde. Pinonaldehyde is one of the most abundant oxidation products from α-pinene, with reported molar yield (sum of gas and particle phase) of 10-19%.[27] Similar to pinonaldehyde, norpinonaldehyde ($C_9H_{14}O_2$) and 2,2-dimethyl-cyclobutyl-1,3-dicarboxaldehyde ($C_8H_{12}O_2$) are suggested as the monomer partners of #25 and #118, which are two SOZs with identification confidence level 2. Their eluting follows the order of 19.80 min (#118) < 20.23 min (#25) < 20.70 min (#1) < 20.97 min (#3), which is also qualitatively consistent with knowledge of their reduced polarity when increasing the molecular weight (MW).

As mentioned before, two organic peroxides (#8 and #15) are known as AAHPs, as they were previously synthesized in our liquid-phase ozonolysis of α-pinene experiments following the addition of cis-pinonic acid and acetic acid respectively.[12] Both two AAHPs show fast reactivity (>10 d^{-1}) with iodide, consistent with their known structures as ROOH. Note that cis-pinonic acid is an example that have both -COOH and C=O functional groups, but the addition of cis-pinonic acid during liquid-phase ozonolysis of α-pinene only leads the formation of AAHP rather than both AAHP and SOZ.[12] This suggests that -COOH group is likely more reactive than C=O when competitively bonding with SCI, if the monomer partner has multiple functional groups. This is also qualitatively consistent with a previous finding on kinetic study of SCI, where the relative rate constant between C13 SCI and some reactants follows the order of water (1) < methanol (22) < 2-propanol (50) < formaldehyde (2700) < formic acid (6700) < heptanoic acid (17000), i.e. the values are normalized to water as shown in brackets.[29] For #52 ($C_{19}H_{30}O_6$), its monomer partner should be $C_9H_{14}O_3$ (MW=170), but there are several MW=170 candidates from the oxidation of α-pinene such as norpinonic acid, pinalic-4-acid and other isomers.[27, 28] Norpinonic acid has both -COOH and C=O functional groups that similar to cis-pinonic acid, which is expected to form AAHP rather than SOZ when boning to SCI. However, #52 shows a peroxide-iodide reactivity of 0.11 d^{-1}, suggesting that it is more likely SOZ. It is therefore we rule out the possibility of MW=170 isomer like norpinonic acid. We tentatively assign this monomer partner as pinalic-4-acid and thus the structure of #52 is suggested at confidence level 3, as we cannot exclude other possible monomers of MW=170.

There are four $C_{20}H_{32}O_6$ (#82, #108, #30, #22) that assigned as SOZs based on their peroxide-iodide reactivity range, which are likely from two different monomers of $C_{10}H_{16}O_3$ (MW=184). There are also several possible candidates for MW184, such as cis-pinonic acid, hydroxy pinonaldehyde, (2,2-dimethyl-3-acetyl)-cyclobutyl formate, etc.[27, 28] Cis-pinonic acid is unlikely given that only AAHP (rather than both AAHP and SOZ) was found in our recent study. 1-hydroxy pinonaldehyde and 10-hydroxy pinonaldehyde are known oxidation product from pinonaldehyde.[28] We tentatively assign 10-hydroxy pinonaldehyde rather than (2,2-dimethyl-3-acetyl)-cyclobutyl formate as the monomer partner of #82 and #108, which elute at earlier RT (18.88 and 19.25 min) compared with #1 and #3 (20.70 and 20.97 min), consistent the increased polarity due to the addition of -OH functional group. However, 1-hydroxy pinonaldehyde could also be possible candidate. Therefore, the structures of #82 and #108 are suggested at confidence level 3. Similarly, we tentatively assign (2,2-dimethyl-3-acetyl)-cyclobutyl formate as the monomer partner of #30 and #22, though other unknown structures of MW=184 may exist. Interestingly, by gathering all information from the three isomeric pairs of SOZs (#1 and #3, #30 and #22, #82 and #108), they show a highly consistent eluting order, e.g. the one with higher k_{1st} value always elutes earlier, with a factor of 2-6 difference in $\tau_{1/e}$. Among the 12 organic peroxides, #5 ($C_{10}H_{18}O_4$) is the most uncertain one, which is expected from bimolecular reaction between C_{10} SCI and H_2O, leading the formation of HAHP that belongs to ROOH. However, the k_{1st} value of #5 (0.042 d^{-1}) does suggest to be a very slowly reactive peroxide, likely belonging to ROOR. Therefore, the structure of #5 is only tentatively assigned with confidence level 3.

Most of these SCI-derived organic peroxides in α-pinene SOA have not been proposed before. We provide solid evidence for elucidation their possible structures by collecting different aspects of information from SOA iodometry kinetics experiments, liquid-phase ozonolysis experiments, and chromatographic eluting and polarity analysis. Some of them are subject to further detailed and accurate structural characterization, e.g. NMR analysis. Nevertheless, the above examples clearly reinforce the fact that the peroxide-iodide reactivity is a useful metric for elucidating the formation pathways and structures of organic peroxide in SOA.

Table 1 Summary of the 12 SCI-derived peroxides identified in α-pinene SOA in this study

Rank #	SCI-derived peroxide	RT	intensity	Perc.	k_{1st}	$\tau_{1/e}$	Monomer partner		SCI-derived peroxide	
		(min)	($\times 10^6$)	(%)	(d^{-1})	(d)	formula	structure	suggested structure*	comments
1	$C_{20}H_{32}O_5$ MW=352	20.70	5.4	5.8	0.16	6.3	$C_{10}H_{16}O_2$ MW=168 pinonaldehyde	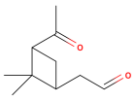	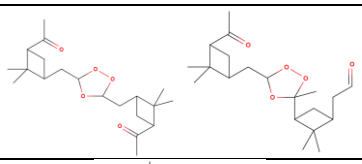	SOZ level 2
3	$C_{20}H_{32}O_5$ MW=352	20.97	5.0	5.4	0.046	21.7				
5	$C_{10}H_{18}O_4$ MW=202	10.08	2.0	2.2	0.042	24.0	H_2O		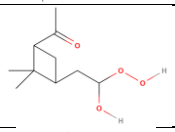	HAHP level 3
15	$C_{12}H_{20}O_5$ MW=244	13.57	1.3	1.4	21.2	0.05	$C_2H_4O_2$ MW=60 acetic acid	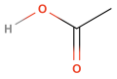	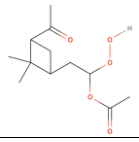	AAHP level 2
8	$C_{20}H_{32}O_6$ MW=368	17.78	1.8	2.0	12.4	0.08	$C_{10}H_{16}O_3$ MW=184 cis-pinonic acid	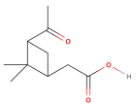	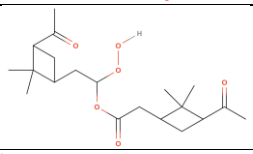	AAHP level 2
82	$C_{20}H_{32}O_6$ MW=368	18.88	0.30	0.3	0.34	3.0	$C_{10}H_{16}O_3$ MW=184 10-hydroxy pinonaldehyde	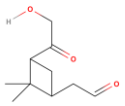	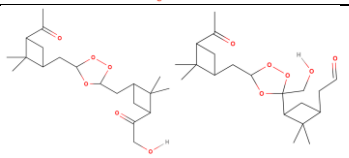	SOZ level 3
108	$C_{20}H_{32}O_6$ MW=368	19.25	0.23	0.2	0.058	17.3				
30	$C_{20}H_{32}O_6$ MW=368	21.73	0.58	0.6	0.22	4.5	$C_{10}H_{16}O_3$ MW=184 (2,2-dimethyl-3-acetyl)-cyclobutyl formate	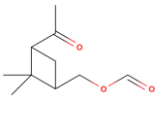	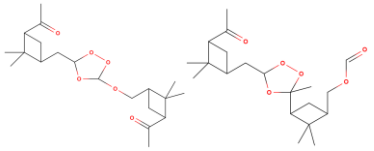	SOZ level 3
22	$C_{20}H_{32}O_6$ MW=368	21.97	0.72	0.8	0.086	11.6				
25	$C_{19}H_{30}O_5$ MW=338	20.23	0.63	0.7	0.044	22.7	$C_9H_{14}O_2$ MW=154 norpinonaldehyde	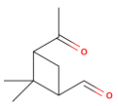	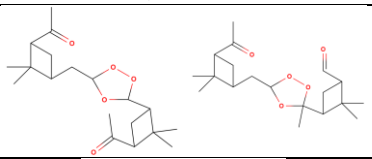	SOZ level 2
52	$C_{19}H_{30}O_6$ MW=354	19.93	0.40	0.4	0.11	9.2	$C_9H_{14}O_3$ MW=170 pinalic-4-acid	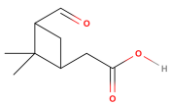	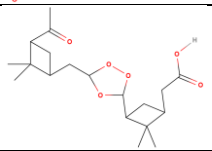	SOZ level 3
118	$C_{18}H_{28}O_5$ MW=324	19.80	0.19	0.2	0.11	9.1	$C_8H_{12}O_2$ MW=140 2,2-dimethyl-cyclobutyl-1,3-dicarboxaldehyde	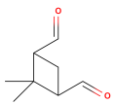	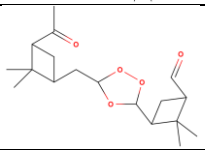	SOZ level 2

*Note: For these suggested structures of SCI-derived organic peroxides, only one C_{10} SCI form is considered in this table, and there should be ×4 different structures given that four different SCI structures [30] are known from the ozonolysis of α-pinene. The identification confidence of level 2 refers to no other possible monomer partner based on the best of our knowledge, and level 3 refers to the existence of other possible monomer partners or other uncertainty.

4 Atmospheric implications

Based on this novel time-dependent iodometry-assisted LC-HRMS and non-targeted analysis, we have accurately identified more than 300 organic peroxides in α-pinene SOA, with diverse range of their reactivity with iodide over four orders of magnitudes. Such diverse peroxide-iodide reactivity suggests their diverse structures, especially a large fraction (>65%) of organic peroxides showing "slow" and "very slow" iodide reactivity with an e-folding lifetime longer than 1 day. For these "very slow" peroxides, they tend to have structures such as R(C=O)OOR or ROOR. This is qualitatively consistent with the reactivity characterization for both commercial peroxides with known structures and some newly proposed structures of SCI-derived organic peroxides (mainly SOZs) identified in α-pinene SOA.

We suggest peroxide-iodide reactivity to be considered as a new metric for future organic peroxide studies with the following two main reasons. Firstly, the peroxide-iodide reactivity is a fundamental chemical property, which provides valuable sub-class structure information for organic peroxide. MS2 and MSn are known to be useful for structure characterization for unknown compounds, which have been applied to SOA studies.[31, 32] However, the long list of structure candidates predicted by MS2 (e.g. SIRIUS, Mass Frontier) is still the main challenging issue. The peroxide-iodide reactivity would be helpful for more accurate structural characterization of organic peroxide, especially to narrow down the candidate structures predicted by MS2 within a more confident range. Secondly, the peroxide-iodide reactivity metric indicates the oxidizing capability of organic peroxide. As shown in Fig. 4, good correlation was found between peroxide-iodide reactivity (determined in this study) and oxidative potential (OP), where the OP data were extracted from the literature [33] for available peroxide standards. Such good correlation between the two independent measurements suggests that peroxide-iodide reactivity might be extrapolated to OP metric in future health assessment, where OP is actually defined by the dithiothreitol (DTT) loss rate from individual redox-active species as a proxy of total oxidative capacity. However, the OP measurement is not the focus of this study, and more experimental evidences are still needed to correlate peroxide-iodide reactivity with peroxide toxicity.

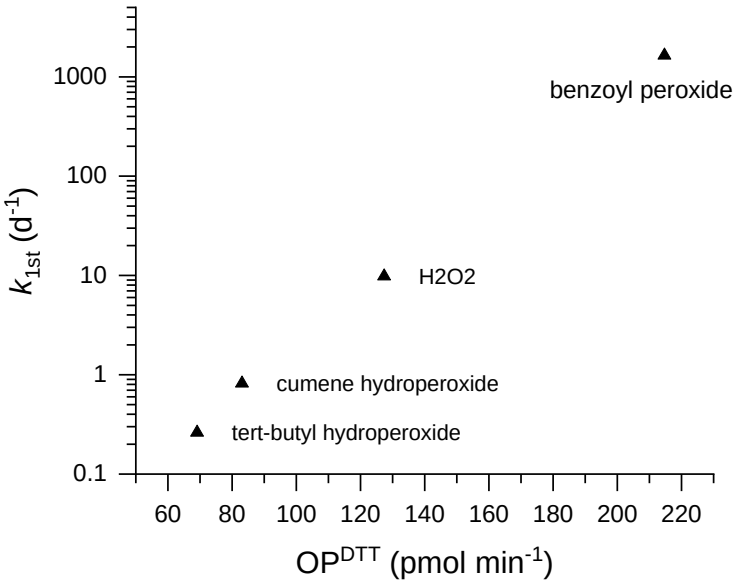

Fig. 4 Correlation between peroxide-iodide reactivity (k_{1st}) and oxidative potential (OP) for four peroxide standards. The OP data made for four peroxide standards were taken from Fig. 3 of Wang et al., (2018),[33] which were experimentally determined by DTT assay.

Another potential implication might be linked to Fenton-like reactions involving organic peroxides. It is known that Fe^{2+} reacts with PAA very fast and its rate constant has been recently determined at 0.1~1×10^5 M^{-1} s^{-1} under pH=3-7,[34] which is 2-3 orders of magnitudes higher than that of H_2O_2 (~77 M^{-1} s^{-1})[35]. This is quite similar to the oxidation of iodide by PAA

and H_2O_2. Very recently, it is shown that PAA and 3-CA can exhibit strong ability to generate OH radicals (the so-called OH burst) when mixing with Fe^{2+} in the bulk solution, while such OH burst is not observed in H_2O_2 and other organic peroxides such as CH, t-BH, etc.[36] Therefore, organic peracids present in aerosol particles likely contribute to the OH burst phenomenon. Such metric of peroxide-iodide reactivity will be useful to further identify some atmospherically important organic peroxides in SOA that are favourable to involve the above Fenton-like reactions, especially leading to the formation of OH radicals with higher yields. These will help to understand the OH sources related to aerosol-cloud chemistry especially in marine environment where irons are abundant.[37, 38]

This novel analytical strategy based on peroxide-iodide reactivity is demonstrated to expand the molecular-level identification capability of organic peroxides in SOA, which offers numerous opportunities to further study their detailed formation and transformation chemistry on a molecular scale. For example, though only α-pinene SOA is investigated in this study, such methodology could be extended to many other SOA systems with different precursors and conditions or even ambient samples. In addition, disentangling the molecular composition of organic peroxides from different reaction pathways could be achieved through well-designed targeted experiments, e.g. by introducing OH, HO_2, RO_2 or SCI scavengers. It should be noted that the iodometry kinetic experiments for α-pinene SOA was performed at 8 ℃ (kept at autosampler) and in the presence of 30 mM acetic acid. We believe such peroxide-iodide reactivity can be accelerated by adjusting the solvent acidity and increasing the temperature. This would allow the whole analytical method to be shortened and therefore not necessarily limited by four weeks as presented in this study. Overall, this study reveals the importance of peroxide-iodide reactivity, which should be a key step for improving our molecular understanding of organic peroxides in atmospheric aerosols in the future.

Acknowledgements

This work was supported by the Swiss National Science Foundation (200021_192192/1). We thank Juliane Krenz for allowing us to use the UV-Vis spectroscopy.

Competing interests

The authors declare that they have no competing interests.

References

(1) Poschl, U. Atmospheric aerosols: composition, transformation, climate and health effects. *Angew Chem Int Ed Engl* **2005**, *44* (46), 7520-7540. DOI: 10.1002/anie.200501122.

(2) Kanakidou, M.; Seinfeld, J. H.; Pandis, S. N.; Barnes, I.; Dentener, F. J.; et al. Organic aerosol and global climate modelling: a review. *Atmospheric Chemistry and Physics* **2005**, *5* (4), 1053-1123. DOI: 10.5194/acp-5-1053-2005.

(3) Zhang, Q.; Jimenez, J. L.; Canagaratna, M. R.; Allan, J. D.; Coe, H.; et al. Ubiquity and dominance of oxygenated species in organic aerosols in anthropogenically-influenced Northern Hemisphere midlatitudes. *Geophysical Research Letters* **2007**, *34* (13). DOI: 10.1029/2007gl029979.

(4) Hallquist, M.; Wenger, J. C.; Baltensperger, U.; Rudich, Y.; Simpson, D.; et al. The formation, properties and impact of secondary organic aerosol: current and emerging issues. *Atmospheric Chemistry and Physics* **2009**, *9* (14), 5155-5236. DOI: 10.5194/acp-9-5155-2009.

(5) Wang, S.; Zhao, Y.; Chan, A. W. H.; Yao, M.; Chen, Z.; et al. Organic Peroxides in Aerosol: Key Reactive Intermediates for Multiphase Processes in the Atmosphere. *Chem Rev* **2023**. DOI: 10.1021/acs.chemrev.2c00430.

(6) Enami, S. Fates of Organic Hydroperoxides in Atmospheric Condensed Phases. *J Phys Chem A* **2021**, *125* (21), 4513-4523. DOI: 10.1021/acs.jpca.1c01513.

(7) Krapf, M.; El Haddad, I.; Bruns, Emily A.; Molteni, U.; Daellenbach, Kaspar R.; et al. Labile Peroxides in Secondary Organic Aerosol. *Chem* **2016**, *1* (4), 603-616. DOI: 10.1016/j.chempr.2016.09.007.

(8) Ye, J.; Abbatt, J. P. D.; Chan, A. W. H. Novel pathway of SO2 oxidation in the atmosphere: reactions with monoterpene ozonolysis intermediates and secondary organic aerosol. *Atmospheric Chemistry and Physics* **2018**, *18* (8), 5549-5565. DOI: 10.5194/acp-18-5549-2018.

(9) Epstein, S. A.; Blair, S. L.; Nizkorodov, S. A. Direct photolysis of alpha-pinene ozonolysis secondary organic aerosol: effect on particle mass and peroxide content. *Environ Sci Technol* **2014**, *48* (19), 11251-11258. DOI: 10.1021/es502350u.

(10) Zhao, R.; Kenseth, C. M.; Huang, Y.; Dalleska, N. F.; Seinfeld, J. H. Iodometry-Assisted Liquid Chromatography Electrospray Ionization Mass Spectrometry for Analysis of Organic Peroxides: An Application to Atmospheric Secondary Organic Aerosol. *Environ Sci Technol* **2018**, *52* (4), 2108-2117. DOI: 10.1021/acs.est.7b04863.

(11) Yao, M.; Li, Z.; Li, C.; Xiao, H.; Wang, S.; et al. Isomer-Resolved Reactivity of Organic Peroxides in Monoterpene-Derived Secondary Organic Aerosol. *Environ Sci Technol* **2022**, *56* (8), 4882-4893. DOI: 10.1021/acs.est.2c01297.

(12) Li, K.; Resch, J.; Kalberer, M. Synthesis and Characterization of Organic Peroxides from Monoterpene-Derived Criegee Intermediates in Secondary Organic Aerosol. *Environ Sci Technol* **2024**. DOI: 10.1021/acs.est.3c07048.

(13) Keller, A.; Kalbermatter, D. M.; Wolfer, K.; Specht, P.; Steigmeier, P.; et al. The organic coating unit, an all-in-one system for reproducible generation of secondary organic matter aerosol. *Aerosol Science and Technology* **2022**, *56* (10), 947-958. DOI: 10.1080/02786826.2022.2110448.

(14) Schmid, R.; Heuckeroth, S.; Korf, A.; Smirnov, A.; Myers, O.; et al. Integrative analysis of multimodal mass spectrometry data in MZmine 3. *Nat Biotechnol* **2023**, *41* (4), 447-449. DOI: 10.1038/s41587-023-01690-2.

(15) Heuckeroth, S.; Damiani, T.; Smirnov, A.; Mokshyna, O.; Brungs, C.; et al. Reproducible mass spectrometry data processing and compound annotation in MZmine 3. *Nat Protoc* **2024**, *19* (9), 2597-2641. DOI: 10.1038/s41596-024-00996-y.

(16) Klassen, N. V.; Marchington, D.; McGowan, H. C. E. H2O2 Determination by the I3- Method and by KMnO4 Titration. *Analytical Chemistry* **1994**, *66* (18), 2921-2925. DOI: 10.1021/ac00090a020.

(17) Fournier, M. C.; Falk, L.; Villermaux, J. A new parallel competing reaction system for assessing micromixing efficiency—Experimental approach. *Chemical Engineering Science* **1996**, *51* (22), 5053-5064. DOI: 10.1016/0009-2509(96)00270-9.

(18) Xiao, J.; Wang, M.; Pang, Z.; Dai, L.; Lu, J.; et al. Simultaneous spectrophotometric determination of peracetic acid and the coexistent hydrogen peroxide using potassium iodide as the indicator. *Analytical Methods* **2019**, *11* (14), 1930-1938. DOI: 10.1039/c8ay02772b.
(19) Zhang, X.; Chen, Z. M.; He, S. Z.; Hua, W.; Zhao, Y.; et al. Peroxyacetic acid in urban and rural atmosphere: concentration, feedback on PAN-NO_x cycle and implication on radical chemistry. *Atmospheric Chemistry and Physics* **2010**, *10* (2), 737-748. DOI: 10.5194/acp-10-737-2010.
(20) Ao, X. W.; Eloranta, J.; Huang, C. H.; Santoro, D.; Sun, W. J.; et al. Peracetic acid-based advanced oxidation processes for decontamination and disinfection of water: A review. *Water Res* **2021**, *188*, 116479. DOI: 10.1016/j.watres.2020.116479.
(21) Awad, M. I.; Oritani, T.; Ohsaka, T. Kinetic studies on the oxidation of iodide by peroxyacetic acid. *Inorganica Chimica Acta* **2003**, *344*, 253-256. DOI: 10.1016/s0020-1693(02)01337-3.
(22) Copper, C. L.; Koubek, E. Kinetics of the molybdate and tungstate catalyzed oxidation of iodide by hydrogen peroxide. *Inorganica Chimica Acta* **1999**, *288* (2), 229-232. DOI: 10.1016/s0020-1693(99)00079-1.
(23) Chen, L.; Pan, H.; Zhai, G.; Luo, Q.; Li, Y.; et al. Widespread occurrence of in-source fragmentation in the analysis of natural compounds by liquid chromatography-electrospray ionization mass spectrometry. *Rapid Commun Mass Spectrom* **2023**, *37* (12), e9519. DOI: 10.1002/rcm.9519.
(24) Giera, M.; Aisporna, A.; Uritboonthai, W.; Siuzdak, G. The hidden impact of in-source fragmentation in metabolic and chemical mass spectrometry data interpretation. *Nat Metab* **2024**, *6* (9), 1647-1648. DOI: 10.1038/s42255-024-01076-x.
(25) Schymanski, E. L.; Jeon, J.; Gulde, R.; Fenner, K.; Ruff, M.; et al. Identifying small molecules via high resolution mass spectrometry: communicating confidence. *Environ Sci Technol* **2014**, *48* (4), 2097-2098. DOI: 10.1021/es5002105.
(26) Bianchi, F.; Kurten, T.; Riva, M.; Mohr, C.; Rissanen, M. P.; et al. Highly Oxygenated Organic Molecules (HOM) from Gas-Phase Autoxidation Involving Peroxy Radicals: A Key Contributor to Atmospheric Aerosol. *Chem Rev* **2019**, *119* (6), 3472-3509. DOI: 10.1021/acs.chemrev.8b00395.
(27) Yu, J.; Cocker Iii, D. R.; Griffin, R. J.; Flagan, R. C.; Seinfeld, J. H. Gas-Phase Ozone Oxidation ofMonoterpenes: Gaseous and Particulate Products. *Journal of Atmospheric Chemistry* **1999**, *34* (2), 207-258. DOI: 10.1023/a:1006254930583.
(28) Jaoui, M.; Kamens, R. M. Gaseous and Particulate Oxidation Products Analysis of a Mixture of α-pinene + β-pinene/O3/Air in the Absence of Light and α-pinene + β-pinene/NOx/Air in the Presence of Natural Sunlight. *Journal of Atmospheric Chemistry* **2003**, *44* (3), 259-297. DOI: 10.1023/a:1022977427523.
(29) Tobias, H. J.; Ziemann, P. J. Kinetics of the Gas-Phase Reactions of Alcohols, Aldehydes, Carboxylic Acids, and Water with the C13 Stabilized Criegee Intermediate Formed from Ozonolysis of 1-Tetradecene. *The Journal of Physical Chemistry A* **2001**, *105* (25), 6129-6135. DOI: 10.1021/jp004631r.
(30) Newland, M. J.; Rickard, A. R.; Sherwen, T.; Evans, M. J.; Vereecken, L.; et al. The atmospheric impacts of monoterpene ozonolysis on global stabilised Criegee intermediate budgets and SO2 oxidation: experiment, theory and modelling. *Atmospheric Chemistry and Physics* **2018**, *18* (8), 6095-6120. DOI: 10.5194/acp-18-6095-2018.
(31) Yasmeen, F.; Szmigielski, R.; Vermeylen, R.; Gomez-Gonzalez, Y.; Surratt, J. D.; et al. Mass spectrometric characterization of isomeric terpenoic acids from the oxidation of alpha-pinene, beta-pinene, d-limonene, and Delta3-carene in fine forest aerosol. *J Mass Spectrom* **2011**, *46* (4), 425-442. DOI: 10.1002/jms.1911.
(32) Müller, L.; Reinnig, M. C.; Warnke, J.; Hoffmann, T. Unambiguous identification of esters as oligomers in secondary organic aerosol formed from cyclohexene and cyclohexene/α-pinene ozonolysis. *Atmospheric Chemistry and Physics* **2008**, *8* (5), 1423-1433. DOI: 10.5194/acp-8-1423-2008.

(33) Wang, S.; Ye, J.; Soong, R.; Wu, B.; Yu, L.; et al. Relationship between chemical composition and oxidative potential of secondary organic aerosol from polycyclic aromatic hydrocarbons. *Atmospheric Chemistry and Physics* **2018**, *18* (6), 3987-4003. DOI: 10.5194/acp-18-3987-2018.
(34) Kim, J.; Zhang, T.; Liu, W.; Du, P.; Dobson, J. T.; et al. Advanced Oxidation Process with Peracetic Acid and Fe(II) for Contaminant Degradation. *Environmental Science & Technology* **2019**, *53* (22), 13312-13322. DOI: 10.1021/acs.est.9b02991.
(35) De Laat, J.; Le Truong, G. Kinetics and modeling of the Fe(III)/H2O2 system in the presence of sulfate in acidic aqueous solutions. *Environ Sci Technol* **2005**, *39* (6), 1811-1818. DOI: 10.1021/es0493648.
(36) Campbell, S. J.; La, C.; Zhou, Q.; Le, J.; Galvez-Reyes, J.; et al. Characterizing Hydroxyl Radical Formation from the Light-Driven Fe(II)–Peracetic Acid Reaction, a Key Process for Aerosol-Cloud Chemistry. *Environmental Science & Technology* **2024**, *58* (17), 7505-7515. DOI: 10.1021/acs.est.3c10684.
(37) Duce, R. A.; Tindale, N. W. Atmospheric transport of iron and its deposition in the ocean. *Limnology and Oceanography* **1991**, *36* (8), 1715-1726. DOI: https://doi.org/10.4319/lo.1991.36.8.1715.
(38) Paulson, S. E.; Gallimore, P. J.; Kuang, X. M.; Chen, J. R.; Kalberer, M.; et al. A light-driven burst of hydroxyl radicals dominates oxidation chemistry in newly activated cloud droplets. *Sci Adv* **2019**, *5* (5), eaav7689. DOI: 10.1126/sciadv.aav7689.